

## Supplementary Materials

### **A novel heterojunction Bi<sub>2</sub>SiO<sub>5</sub>/g-C<sub>3</sub>N<sub>4</sub>: Synthesis, characterization, photocatalytic activity, and mechanism**

Chin-Tsung Yang<sup>a</sup>, Wenlian William Lee<sup>b,c</sup>, Ho-Pan Lin<sup>a</sup>, Yong-Ming Dai<sup>a</sup>, Han-  
Ting Chi<sup>a</sup>, Chiing-Chang Chen<sup>a\*</sup>

<sup>a</sup> Department of Science Education and Application, National Taichung University of  
Education, Taichung 403, Taiwan

<sup>b</sup> Department of Occupational Safety and Health, Chung-Shan Medical University,  
Taichung 402, Taiwan

<sup>c</sup> Department of Occupational Medicine, Chung-Shan Medical University Hospital,  
Taichung 402, Taiwan

\* Author to whom correspondence should be addressed

E-mail: [ccchen@mail.ntcu.edu.tw](mailto:ccchen@mail.ntcu.edu.tw) ; [wlee01@csmu.edu.tw](mailto:wlee01@csmu.edu.tw)

Fax: +886-4-2218-3560

Tel: +886-4-2218-3406/+886-4-24730022

### Separation and Identification of the intermediates

With visible light irradiation, temporal variations occurring in the solution of CV dye during the degradation process were examined by HPLC coupled with a photodiode array detector and ESI mass spectrometry. Given irradiation of CV up to 24 h at pH 3, the chromatograms are illustrated in **Figure S1**, recorded at 580, 350, and 300 nm and nineteen intermediates were identified, with the retention time under 50 min. The CV dye and its related intermediates were denoted as species **A-J**, **a-f**, and  **$\alpha$ - $\gamma$** . Except for the initial CV dye (peak A), the peaks initially increased before subsequently decreasing, indicating the formation and transformation of the intermediates.

In **Figure S2**, the absorption maximum of the spectral bands shifted from 585.5 nm (spectrum A) to 544.5 nm (spectrum J), from 373.5 nm (spectrum a) to 339.0 nm (spectrum f), and from 288.9 nm (spectrum  $\alpha$ ) to 278.2 nm (spectrum  $\gamma$ ). The maximum adsorption in the visible and ultraviolet spectral region of each intermediates are depicted in **Table S1**. They were identified as **A-J a-f**, and  **$\alpha$ - $\gamma$** , respectively corresponding to the peaks A-J, a-f, and  $\alpha$ - $\gamma$  in **Figure S1**. These shifts of the absorption band were presumed to result from the formation of a series of *N*-de-methylated intermediates. From these results, several families of intermediates could be distinguished.

The first family is marked in the chromatogram of **Figure S1(a)** and illustrated in **Figure S2(a)**. The wavelength position of the major adsorption band of intermediates of *N*-de-methylated CV dye moved toward the blue region,  $\lambda_{\max}$ , **A** (CV), 585.5 nm; **B**, 581.2 nm; **C**, 573.9 nm; **D**, 577.5 nm; **E**, 566.5 nm; **F**, 570.2 nm; **G**, 562.9 nm; **H**, 565.9 nm; **I**, 555.5 nm; **J**, 544.5 nm. The *N*-de-methylation of the CV dye caused the wavelength shifts, depicted in **Table S1**, due to an attack by one of the active oxygen species on the *N,N*-dimethyl or *N*-methyl group. It was previously reported that the CV dye was *N*-de-methylated in a stepwise manner (i.e., methyl groups were removed one by one as confirmed by the gradual peak wavelength shifts toward the blue region) and this was confirmed as the **Table S1** shown.

The second family is marked in the chromatogram of **Figure S1(b)** and illustrated in **Figure S2(b)**. The destruction of CV yielded **a**,  **$\alpha$** , and their *N*-de-methylated products *N*-hydroxymethylated intermediates. The wavelength position of the major adsorption band of the *N*-de-methylation of the **a** and the *N*-hydroxymethylated intermediates of the *N*-de-methylated **a** species, produced by cleavage of the CV chromophore ring structure, moved toward the blue region,  $\lambda_{\max}$ , **a**, 373.5 nm; **b**, 366.3 nm; **c**, 362.7 nm; **d**, 362.9 nm; **e**, 357.0 nm; **f**, 339.0 nm. The proposed intermediate (**a**) was compared with a standard material of 4-(*N,N*-dimethylamino)-4'-

(*N,N'*-dimethylamino)benzophenone. The retention time and the absorption spectra were identical.

The third family is marked in the chromatogram of **Figure S1(c)** and illustrated in **Figure S2(c)**. The wavelength position of the major adsorption band of the *N*-demethylation of the ***α***, produced by cleavage of the CV chromophore ring structure, moved toward the blue region,  $\lambda_{\text{max}}$ , ***α***, 288.9 nm; ***β***, 285.3nm; ***γ***, 278.2 nm. The proposed intermediate (***γ***) was compared with the standard material of 4-aminobenzophenone. The retention time and the absorption spectra were identical.

The intermediates were further identified using the HPLC-ESI mass spectrometric method, and the relevant mass spectra are illustrated in **Figures S3** and **Table S1**. The molecular ion peaks appeared in the acid forms of the intermediates. The results of mass spectral analysis confirmed that the component **A** (CV),  $m/z = 372.19$ , **B**,  $m/z = 358.21$ ; **C**,  $m/z = 344.15$ ; **D**,  $m/z = 344.19$ ; **E**,  $m/z = 330.14$ ; **F**,  $m/z = 330.14$ ; **G**,  $m/z = 316.12$ ; **H**,  $m/z = 316.12$ ; **I**,  $m/z = 302.07$ ; **J**,  $m/z = 288.09$ ; **a**,  $m/z = 269.11$ ; **b**,  $m/z = 255.08$ ; **c**,  $m/z = 241.06$ ; **d**,  $m/z = 241.10$ ; **e**,  $m/z = 227.05$ ; **f**,  $m/z = 213.20$ ; ***α***,  $m/z = 137.93$ , in liquid chromatogram.

### Photodegradation mechanisms of CV

In **Figure S4**, the relative distribution of the obtained intermediates was demonstrated and the relative intensities were recorded at the maximum adsorption wavelength for each intermediate, although a quantitative determination of all of the photogenerated intermediates was not achieved owing to the lack of appropriate molar extinction coefficients for them and a lack of reference standards. The distributions of all of the *N*-de-methylated intermediates were related to the initial concentration of CV. Nonetheless, it was clearly observed the changes in the distribution of each intermediate during the photodegradation of CV. The successive appearance of the maximum of each intermediate indicated that the *N*-de-methylation of CV, **a** and ***α***, was a stepwise photochemical process.

Most of the  $\cdot\text{OH}$  radicals were generated directly either from the reaction between the holes and surface-adsorbed  $\text{H}_2\text{O}$  or  $\text{OH}^-$  [1-4]. The *N*-de-methylation of the CV dye occurred mostly through attack by the  $\cdot\text{OH}$  species on the *N,N*-dimethyl group of CV. The degradation intermediates were clearly observed to reach their maximum concentrations (**Figure S4(a)**). The results discussed above can be seen more clearly in **Figure S5**. The degradation of the CV dye occurred mostly through the attack by the  $\cdot\text{OH}$  species on the central carbon portion of CV and produced **a** and ***α***. The degradation intermediates were clearly observed to reach their maximum concentrations (**Figure S4(b)**). The results discussed above can be seen more clearly in **Figure S6**.

In earlier reports [5,6], most *N*-de-alkylation processes were preceded by the formation of a nitrogen-centered radical, while the destruction of dye chromophore structures was preceded by the generation of a carbon-centered radical. Consistently, the degradation of CV must occur via two different photodegradation pathways due to the formation of different radicals. It was no doubt that the  $\cdot\text{OH}$  attack on the dye yielded a cationic radical, which could then undergo hydrolysis and/or follow various deprotonation pathways, which in turn were determined by different adsorption modes of CV on the  $\text{Bi}_2\text{SiO}_5/\text{g-C}_3\text{N}_4$  particles surface.

Based on the above experimental results, the photodegradation pathway was tentatively proposed, **Figure S7**. The dye molecule in the  $\text{Bi}_2\text{SiO}_5/\text{g-C}_3\text{N}_4$  system was adsorbed through the positively-charged diethylamine function. The attraction by one  $\cdot\text{OH}$  radical of a hydrogen atom from the dimethylamine methyl group, and the attack by another  $\cdot\text{OH}$  radical on the diethylamine ultimately resulted in *N*-de-methylation. The mono-de-methylated dye derivative, **B**, could also be adsorbed on the  $\text{Bi}_2\text{WO}_6$  particle surface and was implicated in other similar events ( $\cdot\text{OH}$  radicals attraction and attack, hydrolysis or deprotonation) to yield the bi-de-methylated dye derivatives, **C** and **D**. The *N*-de-methylation process as described above continued until the formation of the completely de-methylated dye, **J**.

In **Figure S7**, the dye molecule in the  $\text{Bi}_2\text{SiO}_5/\text{g-C}_3\text{N}_4$  system was adsorbed through a conjugated structure cleavage of the CV chromophore structure. The attack by  $\cdot\text{OH}$  radical on the conjugated structure yielded a carbon-centered radical, which was subsequently attacked by molecular oxygen to lead ultimately to **a** and  **$\alpha$** . The same process occurred in the *N*-de-methylated dye to produce the *N*-de-ethylated **a** and  **$\alpha$** . The **a** could also be adsorbed on the  $\text{Bi}_2\text{SiO}_5/\text{g-C}_3\text{N}_4$  particle surface and implicated in other similar events ( $\cdot\text{OH}$  radical attraction and attack, hydrolysis or deprotonation, and/or oxygen attack) to yield a mono-*N*-de-methylated derivative, **b**. Moreover, the same process occurred in  **$\alpha$**  to produce  **$\beta$** . The *N*-de-methylation process, as described above, continued until the formation of the completely *N*-de-methylated **a**, **f**, and *N*-de-methylated  **$\alpha$** ,  **$\gamma$** . All the above *N*-de-methylation processes produced a series of *N*-de-hydroxymethylated intermediates by the hydroxylation of the *N*-methyl group. All the intermediates were subsequently mineralized to result in  $\text{NO}_3^-$  and  $\text{CO}_3^{2-}$  [2, 7].

## References

- [1] X. Li, G. Liu, J. Zhao, *New J. Chem.*, 23 (1999) 1193-1196.
- [2] C.C. Chen, C.S. Lu, *Environ. Sci. Technol.*, 41 (2007) 4389-4396.
- [3] C.C. Chen, F.D. Mai, K.T. Chen, C.W. Wu, C.S. Lu, *Dyes Pigm.*, 75 (2007) 434-442.
- [4] J. Zhao, H. Hidaka, A. Takamura, E. Pelizzetti, N. Serpone, *Langmuir*, 9 (1993)

1646-1650.

[5] C.C. Chen, H.J. Fan, J.L. Jan, *J. Phys. Chem. C*, 112 (2008) 11962-11972.

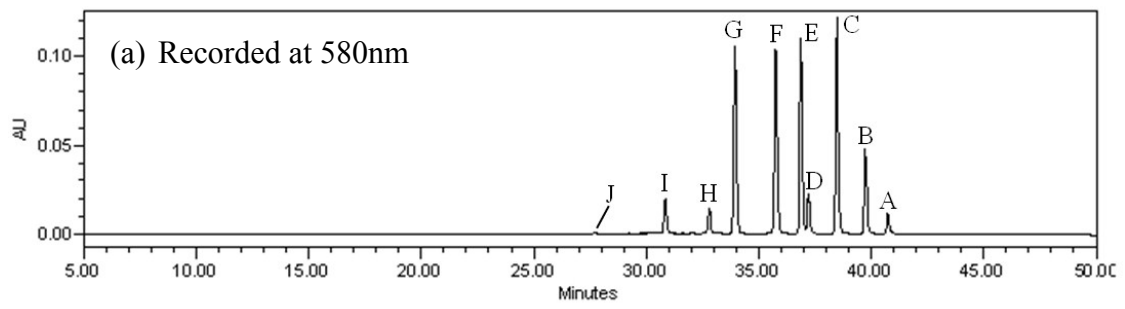
[6] C. Chen, C. Lu, *J. Phys. Chem. C*, 111 (2007) 13922-13932.

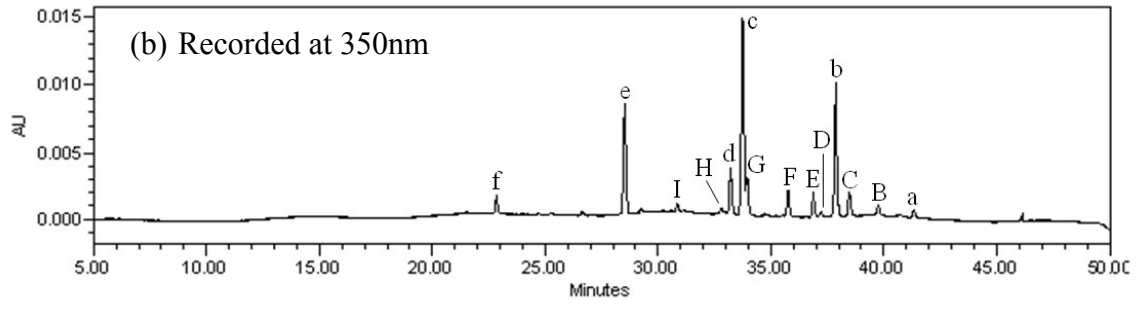
[7] A.B. Prevot, C. Baiocchi, M.C. Brussino, E. Pramauro, P. Savarino, V.

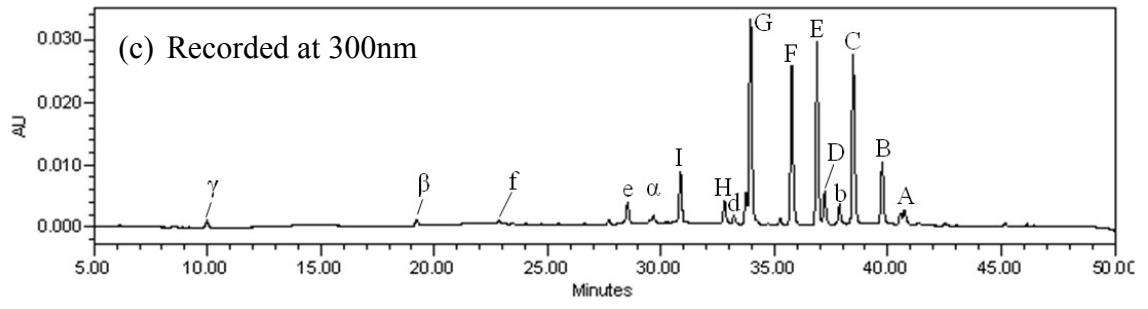
Augugliaro, G. Marci, L. Palmisano, *Environ. Sci. Technol.*, 35 (2001) 971-976.

**Table S1.** Intermediates of the photocatalytic degradation of CV identified by

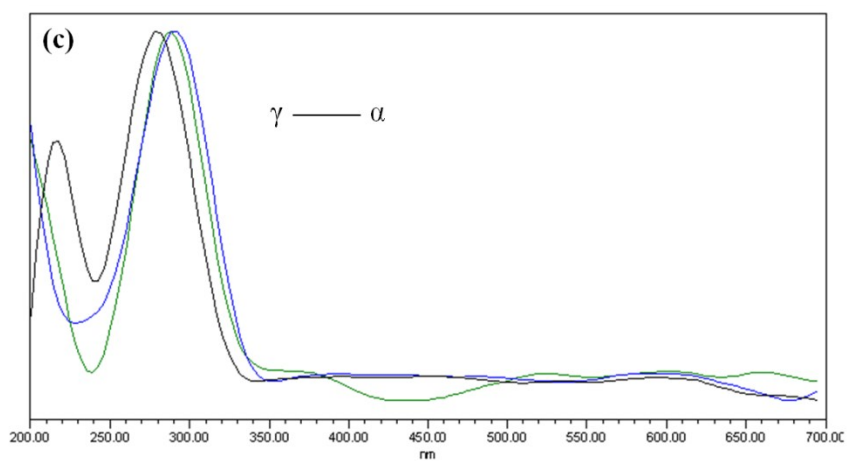
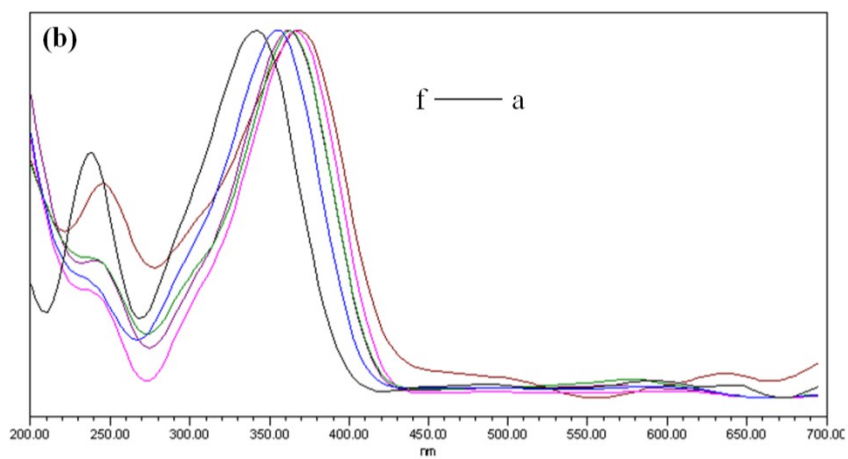
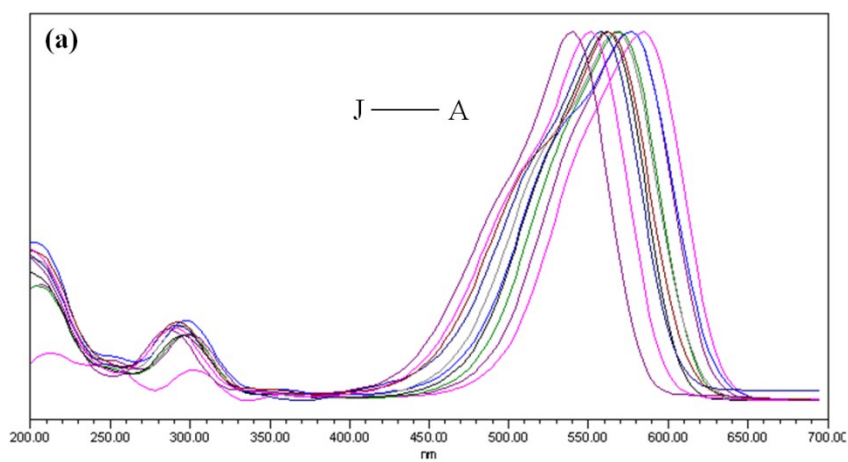
HPLC peaks <sup>o</sup>	Intermediates <sup>o</sup>	Abbreviation <sup>o</sup>	ESI-MS spectrum ions (m/z) <sup>o</sup>	Absorption maximum (nm) <sup>o</sup>	<sup>o</sup>
<b>A</b> <sup>o</sup>	<i>N, N, N', N', N'', N''</i> -hexaethylpararosaniline <sup>o</sup>	CV <sup>o</sup>	372.19 <sup>o</sup>	585.5 <sup>o</sup>	<sup>o</sup>
<b>B</b> <sup>o</sup>	<i>N, N</i> -dimethyl- <i>N', N'</i> -dimethyl- <i>N''</i> -methyl pararosaniline <sup>o</sup>	DDMPR <sup>o</sup>	358.21 <sup>o</sup>	581.2 <sup>o</sup>	<sup>o</sup>
<b>C</b> <sup>o</sup>	<i>N, N</i> -dimethyl- <i>N'</i> -methyl- <i>N''</i> -methylpararosaniline <sup>o</sup>	DMMPR <sup>o</sup>	344.15 <sup>o</sup>	573.9 <sup>o</sup>	<sup>o</sup>
<b>D</b> <sup>o</sup>	<i>N, N</i> -dimethyl- <i>N', N'</i> -dimethyl pararosaniline <sup>o</sup>	DDPR <sup>o</sup>	344.19 <sup>o</sup>	577.5 <sup>o</sup>	<sup>o</sup>
<b>E</b> <sup>o</sup>	<i>N</i> -methyl- <i>N'</i> -methyl- <i>N''</i> -methyl pararosaniline <sup>o</sup>	MMMPR <sup>o</sup>	330.14 <sup>o</sup>	566.5 <sup>o</sup>	<sup>o</sup>
<b>F</b> <sup>o</sup>	<i>N, N</i> -dimethyl- <i>N'</i> -methylpararosaniline <sup>o</sup>	DMPR <sup>o</sup>	330.14 <sup>o</sup>	570.2 <sup>o</sup>	<sup>o</sup>
<b>G</b> <sup>o</sup>	<i>N</i> -methyl- <i>N'</i> -methylpararosaniline <sup>o</sup>	MMPR <sup>o</sup>	316.12 <sup>o</sup>	562.9 <sup>o</sup>	<sup>o</sup>
<b>H</b> <sup>o</sup>	<i>N, N</i> -dimethylpararosaniline <sup>o</sup>	DPR <sup>o</sup>	316.12 <sup>o</sup>	565.9 <sup>o</sup>	<sup>o</sup>
<b>I</b> <sup>o</sup>	<i>N</i> -methylpararosaniline <sup>o</sup>	MPR <sup>o</sup>	302.07 <sup>o</sup>	555.5 <sup>o</sup>	<sup>o</sup>
<b>J</b> <sup>o</sup>	Pararosaniline <sup>o</sup>	PR <sup>o</sup>	288.09 <sup>o</sup>	544.5 <sup>o</sup>	<sup>o</sup>
<b>a</b> <sup>o</sup>	4-( <i>N, N</i> -dimethylamino)-4'-( <i>N', N'</i> -dimethylamino)benzophenone <sup>o</sup>	DDBP <sup>o</sup>	269.11 <sup>o</sup>	373.5 <sup>o</sup>	<sup>o</sup>
<b>b</b> <sup>o</sup>	4-( <i>N, N</i> -dimethylamino)-4'-( <i>N'</i> -methylamino)benzophenone <sup>o</sup>	DMBP <sup>o</sup>	255.08 <sup>o</sup>	366.3 <sup>o</sup>	<sup>o</sup>
<b>c</b> <sup>o</sup>	4-( <i>N</i> -methylamino)-4'-( <i>N'</i> -methylamino)benzophenone <sup>o</sup>	MMBP <sup>o</sup>	241.06 <sup>o</sup>	362.7 <sup>o</sup>	<sup>o</sup>
<b>d</b> <sup>o</sup>	4-( <i>N, N</i> -dimethylamino)-4'-aminobenzophenone <sup>o</sup>	DBP <sup>o</sup>	241.10 <sup>o</sup>	362.9 <sup>o</sup>	<sup>o</sup>
<b>e</b> <sup>o</sup>	4-( <i>N</i> -methylamino)-4'-aminobenzophenone <sup>o</sup>	MBP <sup>o</sup>	227.05 <sup>o</sup>	357.0 <sup>o</sup>	<sup>o</sup>
<b>f</b> <sup>o</sup>	4,4'-Bis-aminobenzophenone <sup>o</sup>	BP <sup>o</sup>	213.20 <sup>o</sup>	339.0 <sup>o</sup>	<sup>o</sup>
<b>α</b> <sup>o</sup>	4-( <i>N, N</i> -dimethylamino)phenol <sup>o</sup>	DAP <sup>o</sup>	137.93 <sup>o</sup>	288.9 <sup>o</sup>	<sup>o</sup>
<b>β</b> <sup>o</sup>	4-( <i>N</i> -methylamino)phenol <sup>o</sup>	MAP <sup>o</sup>	N/A <sup>o</sup>	285.3 <sup>o</sup>	<sup>o</sup>
<b>γ</b> <sup>o</sup>	4-aminophenol <sup>o</sup>	AP <sup>o</sup>	N/A <sup>o</sup>	278.2 <sup>o</sup>	<sup>o</sup>



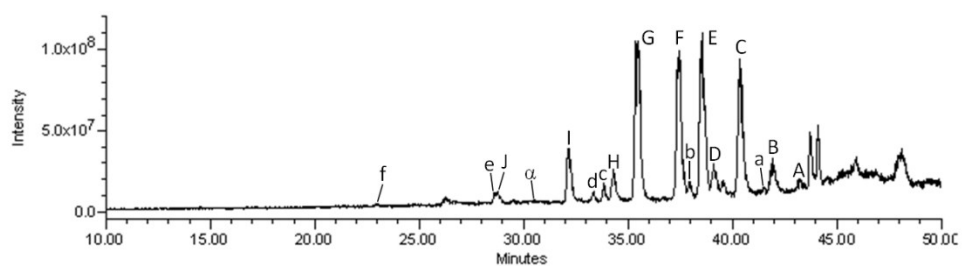




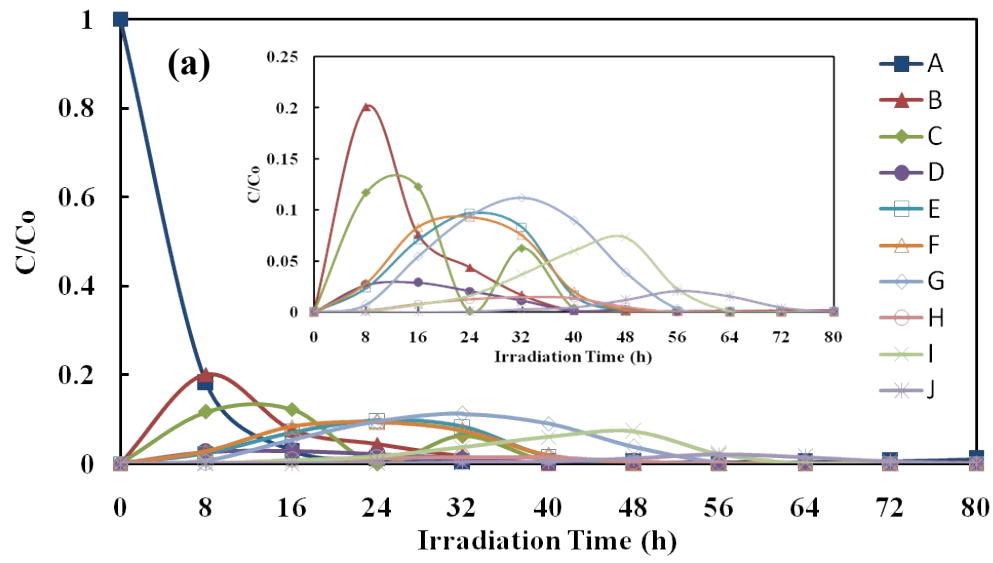
**Figure S1.** HPLC chromatogram of the degraded intermediates at different irradiation intervals, recorded at (a)580 nm (b)350nm (c)300nm.



**Figure S2.** Absorption spectra of the intermediates formed during the photodegradation process of the CV dye corresponding to the peaks in the HPLC chromatograph.



**Figure S3.** Total ion chromatogram of the photodegraded intermediates with photocatalyst dispersions at pH 9 under 16 h irradiation.





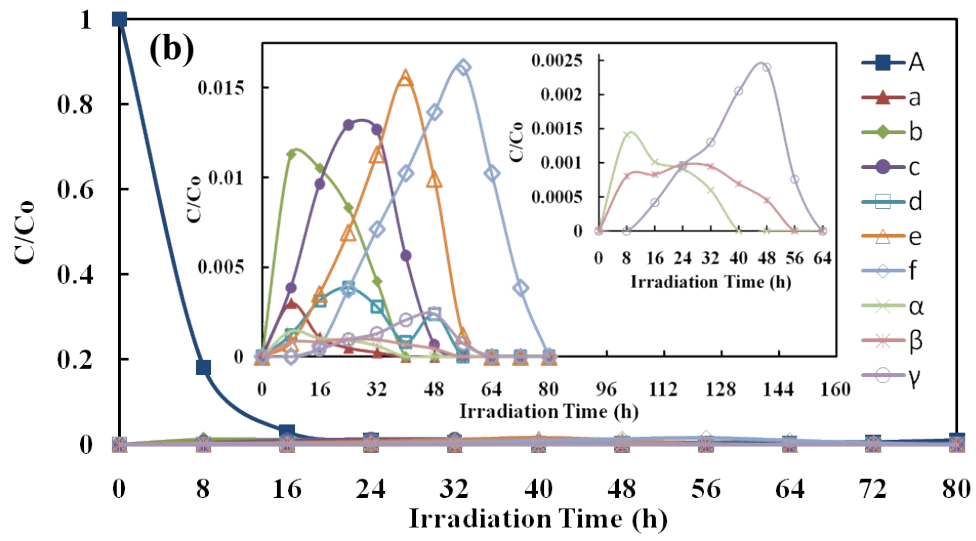


**Figure S4.** Variations in the relative distribution of the intermediates obtained from the photodegradation of CV as a function of irradiation time.

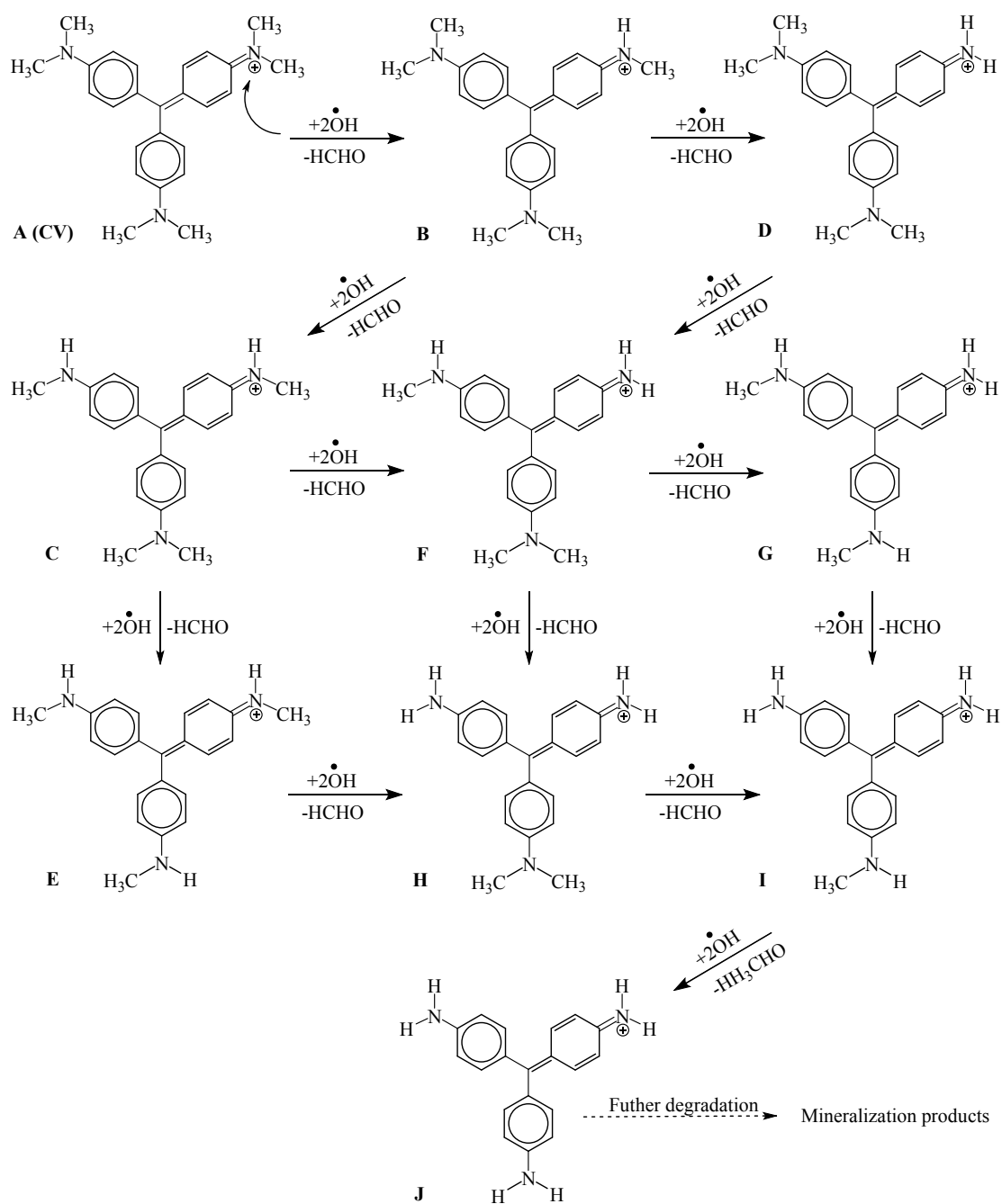


**Figure S5.** Proposed *N*-de-methylation pathway of the CV dye.

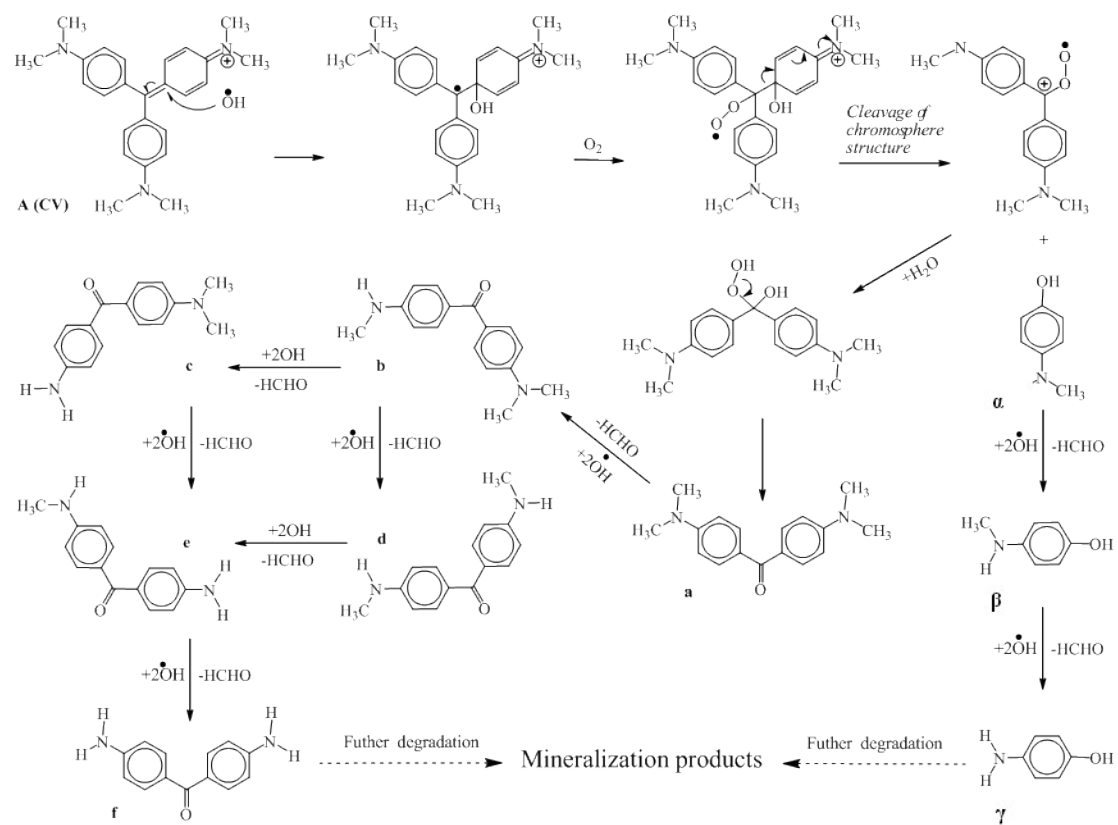


**Figure S6.** Proposed pathway of the destruction of the conjugated structure of the CV dye.

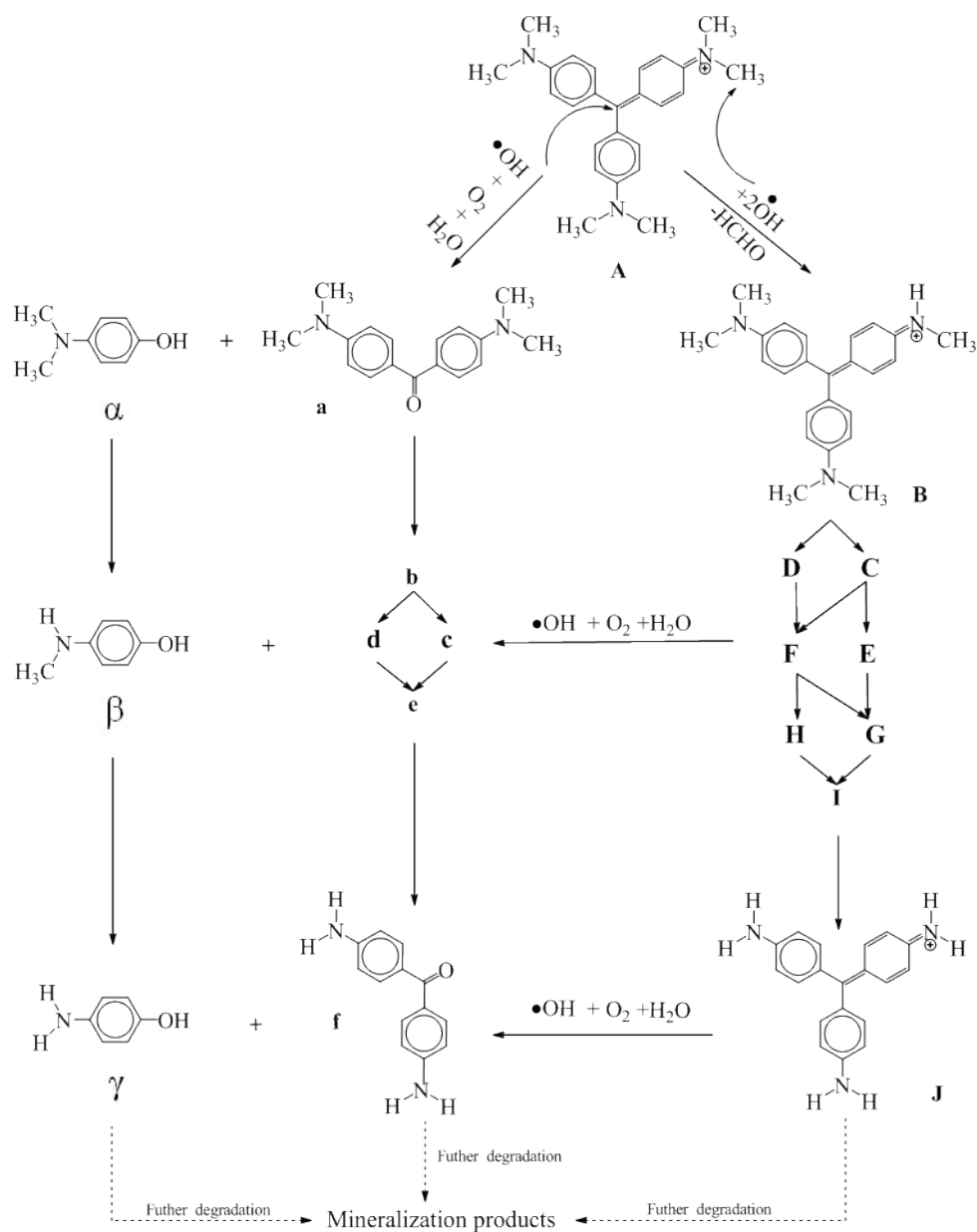


**Figure S7.** Proposed photodegradation mechanism of the CV dye.